The Preparation of Colloidally Stable, Water-Soluble, Biocompatible, Semiconductor Nanocrystals with a Small Hydrodynamic Diameter

Emma E. Lees,[†,‡] Tich-Lam Nguyen,[†] Andrew H. A. Clayton,[‡] and Paul Mulvaney[†,*]

[†]School of Chemistry and Bio21 Institute, University of Melbourne, Parkville, VIC 3010, Australia, and [‡]Ludwig Institute for Cancer Research, PO Box 2008, Royal Melbourne Hospital, VIC 3050, Australia

ABSTRACT We report a simple, economical method for generating water-soluble, biocompatible nanocrystals that are colloidally robust and have a small hydrodynamic diameter. The nanocrystal phase transfer technique utilizes a low molecular weight amphiphilic polymer that is formed *via* maleic anhydride coupling of poly(styrene-*co*-maleic anhydride) with either ethanolamine or Jeffamine M-1000 polyetheramine. The polymer encapsulated water-soluble nanocrystals exhibit the same optical spectra as those formed initially in organic solvents, preserve photoluminescence intensities, are colloidally stable over a wide pH range (pH 3—13), have a small hydrodynamic diameter, and exhibit low levels of nonspecific binding to cells.

KEYWORDS: quantum dots · water-soluble · biocompatible · amphiphilic polymer · PEG · hydrodynamic diameter · cell staining

Semiconductor nanocrystals have found numerous applications in biological assays as fluorescent probes.[1−8] When using nanocrystals for biological applications, control of the chemistry at the nanocrystal surface is of fundamental importance. Quantum dots (QDs) are typically synthesized in high boiling point, nonpolar organic solvents to obtain high quality, monocrystalline particles with narrow size distributions. Following synthesis QDs are stabilized by hydrophobic ligands.[9−13] To disperse QDs in aqueous solvents it is necessary to manipulate the surface chemistry. The ideal biocompatible QD must be homogeneously dispersed and colloidally stable in aqueous solvents, exhibit pH and salt stability, show low levels of nonspecific binding to biological components, maintain a high quantum yield, and have a small hydrodynamic diameter (HD). It has proved extremely difficult to achieve each of these characteristics simultaneously. As a result, over the past 10 years, since the first experiments demonstrating the use of QDs as biological probes,[12] much of the literature has focused on improvements to the surface chemistry of biocompatible nanocrystals. Three main techniques for generating biocompatible nanocrystals have evolved: (i) ligand exchange, (ii) silica encapsulation, and (iii) polymer encapsulation.

Ligand exchange phase transfer techniques replace hydrophobic with hydrophilic ligands on the QD surface. Hydrophobic ligands bind to metal atoms on the QD surface typically through carboxyl, amine, or phosphine oxide groups. To drive hydrophilic ligands onto the QD surface it is necessary that they have a terminal binding group with a high affinity for the QD surface atoms. As mercapto groups have the highest binding affinity for the QD surface, mercapto terminated hydrophilic ligands have been the primary candidates for generating water-soluble QDs. Initially short chain mercapto-alkyl-carboxyl ligands (*e.g.*, mercaptoacetic acid,[2,14] mercaptopropionic acid,[15,16] mercaptoundecanoic acid,[17,18] dihydrolipoic acid (DHLA))[19,20] were used to yield water-soluble QDs. These ligands however rely on electrostatic stabilization, requiring the solvent exposed carboxyl groups to be ionized. This limits their pH and salt stability to basic buffers with low ionic strength. Mercapto-poly(ethylene glycol) (PEG) derivatives, in particular DHLA-PEG,[21−23] have subsequently become the ligand of choice. The ether groups which form the backbone of the PEG chains do not rely on electrostatic interactions for water solubility, but instead utilize hydrogen bonding and steric stabilization. As a result PEG-based ligands confer water solubility over a wide pH range even at high salt concentrations.[21,22] Importantly PEG- functionalized QDs also exhibit reduced

*Address correspondence to mulvaney@unimelb.edu.au.

Received for review February 12, 2009 and accepted April 17, 2009.

Published online April 23, 2009.
10.1021/nn900144n CCC: $40.75

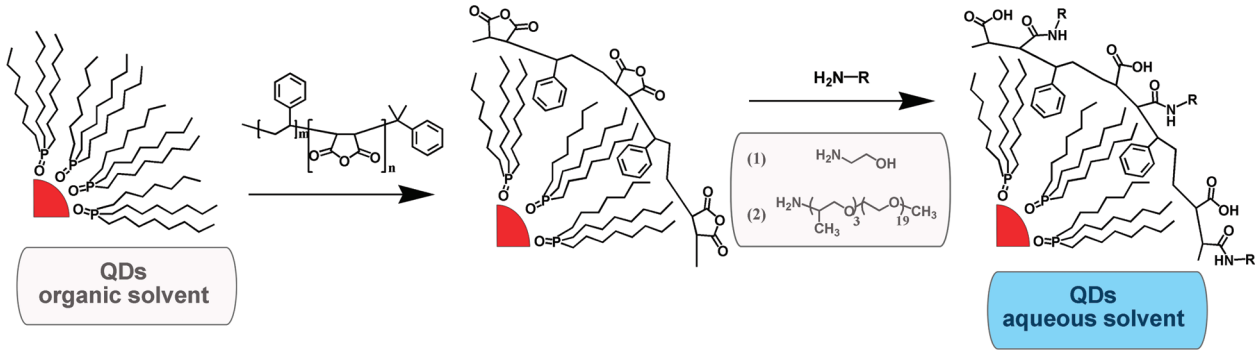

Figure 1. Schematic diagram showing the steps involved to prepare water-soluble QDs using PSMA. PSMA was added to CdSe/ZnS QDs capped with hydrophobic ligands in $CHCl_3$. An amine-terminated ligand, NH_2-R, was added to PSMA capped QDs in $CHCl_3$ to ring open the maleic anhydride groups and generate the amphiphilic polymer coating. The resulting QDs coated with amphiphilic PSMA are soluble in aqueous media. The central box highlights the structures of the two amine terminated ligands used in this study (1) ethanolamine and (2) Jeffamine M1000 polyetheramine.

nonspecific binding to biological components, reduced cellular toxicity, and increased circulation times.[6,24]

While dithiol moieties (such as those present in DHLA) exhibit greater colloidal stability than monothiols, it is difficult to generate water-soluble QDs with a long shelf life using this method. This has been attributed to oxidation of the thiol ligands to disulfides.[17] Another drawback is that while thiol groups are optimal for replacing hydrophobic ligands and minimizing ligand desorption, thiols quench QD photoluminescence.[25,26] This is reduced by using core/shell QDs; however, the ligand exchange technique itself exposes the QD surface to water and oxygen species which also act to quench the QD photoluminescence. In summary, although the ligand exchange phase transfer technique generates water-soluble QDs with the lowest possible hydrodynamic diameter, the photoluminescence is compromised and the long-term colloidal stability remains questionable.

Silica encapsulation involves ligand exchange with silica precursors, such as mercaptopropyltris(methyloxy)silane (MPS), aminopropyltris(methyloxy)silane (APS), or poly(vinylpyrrolidone (PVP), which are then cross-linked to form a silica shell around the QD to impart solubility in aqueous environments.[1,27,28] By physically protecting the QD from the external environment, silica-coated QDs exhibit improved photostability.[29] Notably the silica shell may be functionalized to incorporate PEG chains for improved colloidal stability and biocompatibility. However the growth of a thin, uniform silica shell that encapsulates a single QD is at present nontrivial.

Polymer encapsulation with amphiphilic polymers[5,30−33] or micelles[3] has also been used to transfer QDs into aqueous environments. The main advantage with this approach is that the original hydrophobic ligands are retained on the QD surface. The hydrophobic portion of the polymer intercalates with the hydrophobic ligands on the QD surface leaving the hydrophilic portion of the polymer exposed to solution. By circumventing the need for any direct ligand exchange at the QD surface, polymer encapsulated QDs have the highest reported photoluminescence in water. As with previous techniques, the polymer may be functionalized to include PEG chains to impart colloidal stability and biocompatibility. While polymer stabilized QDs show superior colloidal stability and good retention of photoluminescence intensity, the polymers most conducive to particle stabilization are often not commercially available and functionalized PEG derivatives are expensive. To combat these shortcomings, Yu *et al.* employed poly(maleic anhydride-alt-1-octadecene) (PMAO), a polymer which relies on maleic anhydride coupling with primary amine derivatives to generate an amphiphilic polymer.[32] These authors devised a reaction scheme using cheaper underivatized mPEG-OH to generate PMAO-PEG. However, we found this phase transfer route difficult to reproduce. We also note that the large molecular weight of PMAO (30000−50000 g/mol) substantially increases the QD hydrodynamic diameter.

Here we report a polymer encapsulation nanocrystal phase transfer technique that utilizes a low molecular weight polymer, poly(styrene-co-maleic anhydride) (PSMA, 1700 g/mol). The amphiphilic polymer is formed using either ethanolamine (EA) or Jeffamine M-1000 polyetheramine (M1000), a cheap commercially available amino-PEG derivative, to ring open the maleic anhydride moiety. This simple, low cost method combines the benefits of amphiphilic polymer phase transfer, that is, retaining QD photoluminescence and colloidal stability, while minimizing the hydrodynamic diameter of the final particle.

This procedure is far simpler than the polymer encapsulation processes recently presented by Pellegrino *et al.*[30] and by Anderson and colleagues.[34] Both their approaches involve extensive synthesis or postphase-transfer modifications, while the protocol described here involves spontaneous transfer of the nanocrystals.

RESULTS AND DISCUSSION

QD PSMA Phase Transfer. PSMA, prior to being functionalized to an amphiphile, is soluble in organic solvents.

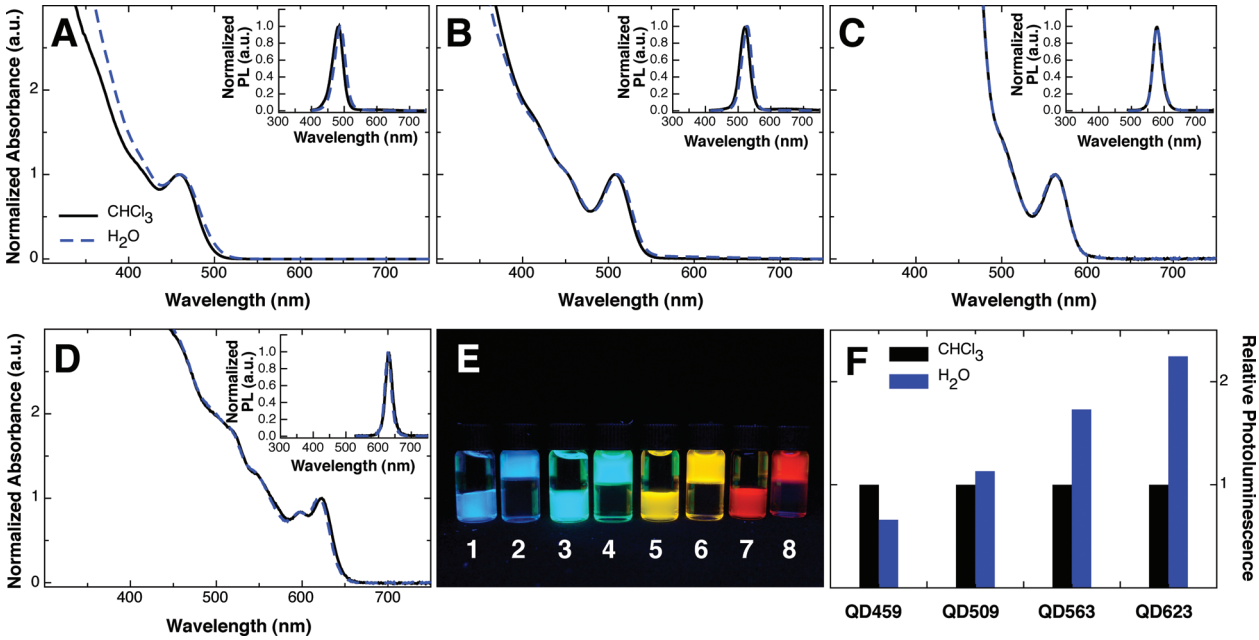

Figure 2. (A−D) Normalized absorbance and photoluminescence (inset) spectra of four different-sized CdSe/ZnS QD samples in $CHCl_3$ and in water capped with PSMA/EA. (E) Fluorescence image of the four QD samples in $CHCl_3$ (vials 1, 3, 5, 7) and in water (vials 2, 4, 6, 8). Samples were excited with a hand-held UV lamp at 365 nm. (F) Relative photoluminescence intensities of the four QD samples in water compared with $CHCl_3$.

We found the most efficient and reproducible phase transfer method was to introduce PSMA to QD samples in $CHCl_3$ and then to convert PSMA to an amphiphile using either EA or M1000 to ring open the maleic anhydride moiety forming a carboxylic acid and an amide linkage to the ring-opening agent (Figure 1). QDs capped with amphiphilic PSMA could then be transferred into water. Other primary amines, including aminobutanol and 2-(2-aminoethoxy)ethanol, were also successfully used as ring-opening agents; however, the discussion in this manuscript will be limited to EA and M1000. This transfer protocol was much simpler and more reproducible than first forming the PSMA amphiphile and then capping the QDs.

Ethanolamine as a Ring-Opening Agent. Figure 2, panels A−D, show normalized absorbance and photoluminescence (inset) spectra of four CdSe/ZnS QD samples with first absorption maxima of 459, 509, 563, and 623 nm, respectively, in $CHCl_3$ and transferred into water with PSMA using EA as the ring-opening agent. The spectra of QDs in water match the original coated QDs in $CHCl_3$ indicating no nanoscale aggregation or surface degradation upon phase transfer. Figure 2E shows a fluorescence image of the four QD samples coated with the original ligands in $CHCl_3$ (vials 1, 3, 5, 7) and capped with PSMA/EA in water (vials 2, 4, 6, 8). The photoluminescence intensities in water were compared to those in $CHCl_3$ (Figure 2F). The optical densities for each sample in $CHCl_3$ and in water were matched at their excitation wavelengths in order to be able to directly compare the photoluminescence intensities of the two samples. The smallest QD sample, QD459, showed a reduction in photoluminescence intensity of 34% upon transfer into water. However for the three remaining samples, QD509, QD563, and QD623, the photoluminescence intensities in water were greater than in $CHCl_3$, with an increase of 13%, 73%, and 125%, respectively. Amines are known to provide additional passivation to QDs, resulting in increased emission intensities.[26] Consequently, we attribute the observed photoluminescence enhancement to the amine groups on the EA interacting directly with the QD surface. This result shows remarkable preservation of QD optical properties upon transfer into water using PSMA/EA.

Jeffamine M-1000 as a Ring-Opening Agent. It has almost become a requirement for biocompatible QDs to incorporate PEG chains into the surface coatings. PEG-functionalized nanocrystals are colloidally stable over a wide pH range and at high salt concentrations. PEG also has the ability to reduce nonspecific binding to biological components, minimize cellular toxicity, and increase circulation times. To functionalize QD surface coatings with PEG chains it is often necessary for the PEG ligands themselves to be functionalized. Carboxyl-, amine-, and thiol-terminated PEG derivatives are among the most common. Unlike underivatized PEGs, α, ω-PEG derivatives are often difficult to synthesize and purify. Jeffamine M-1000 polyetheramine is a cheap, commercially available, low molecular weight amino-PEG derivative (bifunctionalized derivatives are also available). The terminal amino group acts as a nucleophile to spontaneously ring open the maleic anhydride groups on PSMA.

Figure 3A shows normalized absorbance spectra of CdSe/ZnS QD samples with first absorption maxima of 582 nm in $CHCl_3$ and transferred into water with PSMA

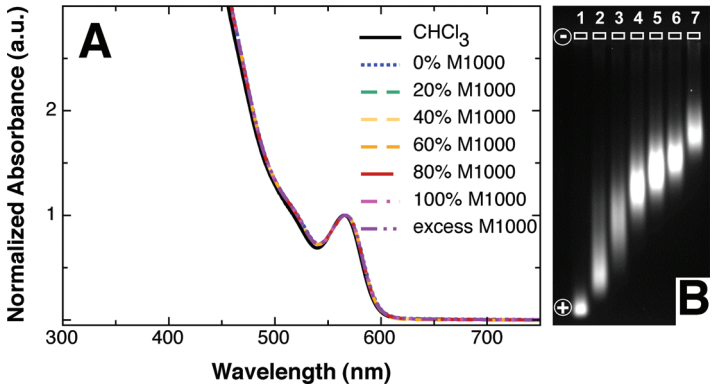

Figure 3. (A) Normalized absorbance spectra of CdSe/ZnS QDs in $CHCl_3$ and in water capped with PSMA with different ratios of M1000:MA groups. The remaining MA groups were ring-opened with EA. (B) Gel shift of QD/PSMA samples with different ratios of M1000 in 1% agarose gel buffered with 1× TBE buffer: (1) 0% M1000 (100% EA), (2) 20% M1000, (3) 40% M1000, (4) 60% M1000, (5) 80% M1000, (6) 100% M1000, (7) excess M1000.

using different ratios of M1000:MA groups. For each sample the remaining maleic anhydride groups were ring opened with EA. As with the QD PSMA/EA samples (Figure 2A−D) the spectra of QDs capped with PSMA/M1000 in water match the original coated QDs in $CHCl_3$ indicating no nanoscale aggregation or surface degradation upon phase transfer. Electrophoretic separation of the QD PSMA/M1000 samples in a 1% agarose gel shows a direct correlation between the ratio of M1000:EA used to ring open the maleic anhydride groups and the QD electrophoretic mobility (Figure 3B). QDs capped with PSMA/EA, that, is, 0% M1000, migrate furthest toward the positive electrode (lane 1). As increasing amounts of M1000 were doped into the surface coating the electrophoretic mobility of the QDs systematically decreased (lanes 2−7).

A reduction in electrophoretic mobility may be attributed to either an increase in hydrodynamic volume (molecular weight) or to a reduction in net surface charge. It is important to note that the number of QD surface charges is not affected by the choice of ring-opening agent. Both EA and M1000 are uncharged. The only contribution to the surface charge arises from carboxylic acid groups associated with the maleic anhydride moieties. As evident from the linear relationship between electrophoretic mobility and M1000 ratio, the observed reduction in electrophoretic mobility may simply be attributed to the increase in hydrodynamic volume with increasing ratios of M1000. The data presented in Figure 3 shows that we are able to systematically control the QD surface chemistry by doping in stoichiometric quantities of M1000.

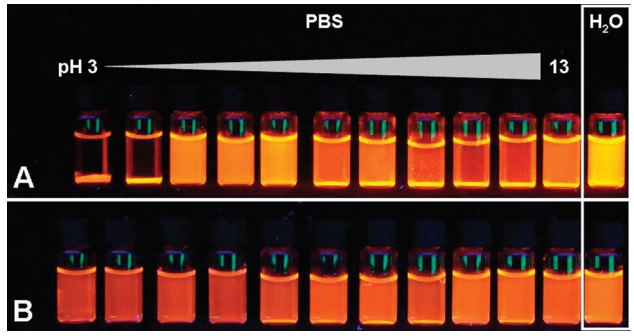

Figure 4. Fluorescence image set of 598 nm emitting CdSe/ZnS QDs capped with (A) PSMA/EA and (B) PSMA/M1000 (M1000 100%) in PBS at various pH values after 7 days at room temperature. For each series a sample in water is shown as a reference (boxed). Samples were excited using a hand-held UV lamp at 365 nm.

TABLE 1. Hydrodynamic Diameter of CdSe/ZnS QD Samples with First Absorption Maxima of 551 nm Capped with Different Surface Chemistries[a].

surface chemistry	HD (nm)
DHLA-PEG	14.8 ± 2.8
PSMA/EA	13.4 ± 3.4
PSMA/M1000	17.8 ± 4.3
PMAO/EA	24.5 ± 8.2

[a]Data were obtained from DLS measurements. Standard deviations are shown.

Colloidal Stability. Figure 4 shows fluorescence images of 598 nm emitting CdSe/ZnS QD samples transferred into water with either (A) PSMA/EA or (B) PSMA/M1000 (100% M1000) diluted into PBS solutions with pH values ranging from 3−13, where the pH was adjusted using either HCl or NaOH. Images were taken 7 days after dilution into the PBS solutions with specified pH values.

The QD PSMA/EA samples at pH 5−7 exhibit colloidal stability as evident from the homogeneous fluorescence of the samples. At high pH values (pH 8−13) there is evidence of colloidal instability seen by the brighter band of fluorescence at the bottom of each vial, and at low pH values (pH 3 and 4) the QD PSMA/EA samples have lost all stability as they have aggregated and crashed out of solution. This result demonstrates that the PSMA amphiphile alone (PSMA/EA) relies at least partially on the carboxyl groups being ionized to electrostatically stabilize the QDs. At low pH values, when the carboxyl groups are protonated the polymer no longer confers colloidal stability to the QDs. Interestingly at high pH values the QD PSMA/EA samples showed early signs of instability, even though in this pH range the carboxyl groups are ionized. It is difficult to rationalize this observation other than to say it is unlikely this instability is caused by electrostatic coupling of free amines to the carboxyl groups as the QD samples have been purified using ultracentrifugal devices to remove excess ligands, including free ethanolamine.

The QD PSMA/M1000 samples on the other hand remain stable across all pH values (pH 3−13) showing no signs of aggregation. Incorporation of M1000 extends the pH range over which the QDs are stable. This indicates that the QD dispersion no longer relies on electrostatic stabilization from the PSMA, but rather is stabilized by the PEG chains. It is noteworthy that QDs

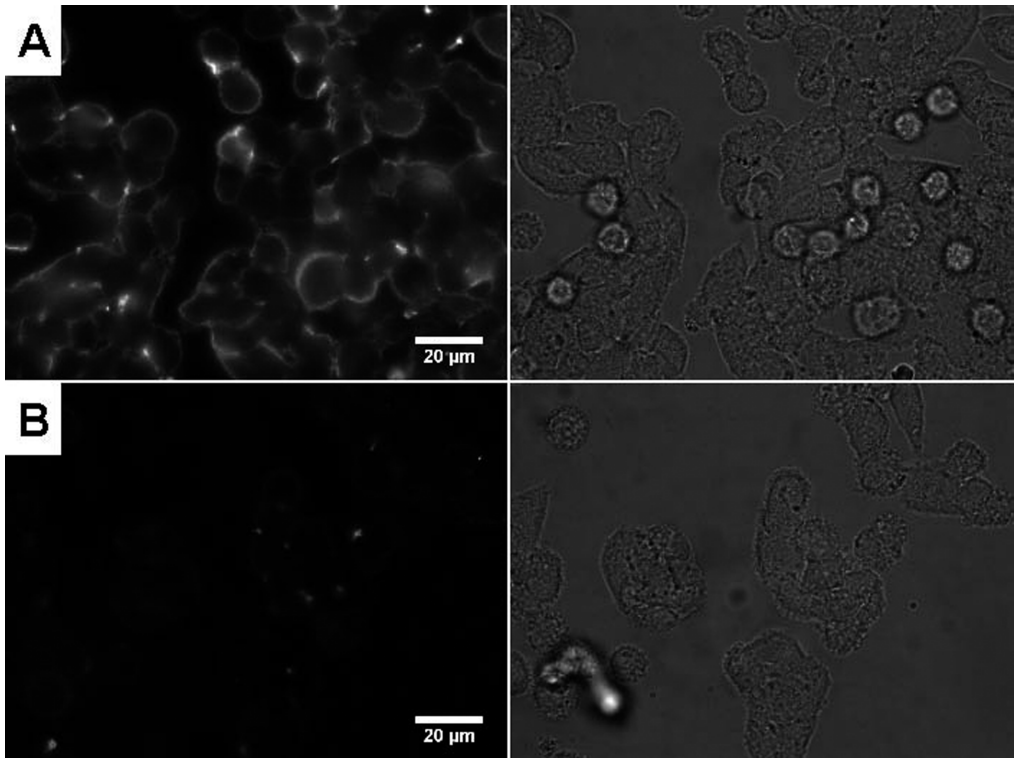

Figure 5. Representative fluorescence (left) and bright field (right) images of fixed LIM1215 cells stained with a 1 μM solution of 592 nm emitting CdSe/ZnS QDs capped with (A) PSMA/EA and (B) PSMA/M1000 (M1000 100%).

capped with PSMA/M1000 dispersed in water exhibit long-term stability, having been stored for up to 6 months with no signs of aggregation.

Hydrodynamic Diameter. The hydrodynamic diameter obtained from DLS measurements of CdSe/ZnS QD samples with first absorption maxima of 551 nm transferred into PBS with either (i) DHLA-PEG, (ii) PSMA/EA, (iii) PSMA/M1000 (100% M1000), or (iv) PMAO/EA are listed in Table 1. QDs coated with PSMA/EA exhibit a similar HD to those capped with DHLA-PEG, 13.4 ± 3.4 and 14.8 ± 2.8 nm, respectively. Incorporation of M1000 into the polymer surface coating slightly increased the HD to 17.8 ± 4.3 nm. Conversely, capping the QDs with PMAO/EA significantly increased the HD to 24.5 ± 8.2 nm. One of the main drawbacks until now of using amphiphilic polymer encapsulation of nanocrystals has been the significant increase to the QD hydrodynamic diameter. This is due to the bilayer created when using an amphiphilic polymer (the original hydrophobic ligands plus the polymer shell) and the high molecular weight polymers that have been used (PMAO, 30000−50000 g/mol). The data presented here clearly demonstrate that QDs capped with a low molecular weight amphiphilic polymer can achieve a hydrodynamic diameter as low as the ligand exchange method. This is vital for the use of QDs in *in vivo* studies, as diagnostic and therapeutic agents where QD biodistribution and renal clearance are highly sensitive to hydrodynamic diameter.[35]

These particles present the smallest hydrodynamic diameter for polymer encapsulated QDs to date, while maintaining the monodispersity of the semiconductor nanocrystals. Smith *et al*. have very recently outlined a novel synthetic route for generating water-soluble QDs;[36] while it leads to small hydrodynamic diameters, the nanocrystals themselves are synthesized *in situ* and do not have the monodispersity achieved through current nonaqueous routes.

Nonspecific Binding. An important requirement for biocompatible QDs is that they display minimal nonspecific binding to biological components. That way when a protein, antibody, or DNA oligomer of interest is attached to a QD the background contribution from nonspecifically bound QDs is minimized. Figure 5 shows fluorescence (left) and bright field (right) images of fixed LIM1215 human carcinoma cells stained with a 1 μM solution of 592 nm emitting QDs capped with (A) PSMA/EA and (B) PSMA/M1000 (100% M1000). The QD PSMA/EA sample shows a high level of nonspecific binding to the cells as seen by the strong fluorescence associated with the cells. Conversely, the QD PSMA/M1000 sample shows negligible nonspecific binding as seen by the minimal cellular associated fluorescence. This result is in agreement with previous reports which have found that on the one hand charged QDs exhibit high levels of nonspecific binding to cell surfaces. However the nonspecific binding is subsequently reduced when the QD surface is functionalized with uncharged PEG.[23,24]

CONCLUSION

Encapsulating QDs in amphiphilic polymers is a well-established method for generating biocompatible QDs. However incorporating PEG chains into the polymer surface coating has previously been either costly or nontrivial, and the hydrodynamic diameter of the final water-soluble QD has been significantly increased using this method. This drastically reduces the viability of QD labeling in *in vivo* studies. We have developed an amphiphilic polymer phase transfer scheme that (i) utilizes a cheap amino-PEG derivative to functionalize the polymer for improved colloidal stability and biocompatibility and (ii) minimizes the hydrodynamic diameter of the final QD particle to a size comparable to those obtained using direct ligand exchange techniques. These improvements to the amphiphilic polymer phase transfer route have enabled us to design the ideal biocompatible QD. QDs functionalized with PSMA/M1000 exhibit the same optical spectra as those formed initially in organic solvents, are colloidally robust, exhibit low levels of background fluorscence, have a small hydrodynamic diameter, and are equipped with a carboxyl group for conjugation to proteins, antibodies, or DNA oligomers.

METHODS

Materials. Poly(styrene-*co*-maleic anhydride) terminated with cumene (PSMA, ~1700 g/mol), poly(maleic anhydride-alt-1-octadecene) (PMAO, ~30000−50000 g/mol), phosphonoacetic acid (PsAA, 98%), tetramethylammonium hydroxide (TMAOH, 25 wt % in methanol), paraformaldehyde (PFA, 95%), and bovine serum albumin (BSA, 98%) were purchased from Sigma-Aldrich. Jeffamine M-1000 polyetheramine (M1000, 1000 g/mol) was purchased from Huntsman. Ethanolamine (EA, 97%) was purchased from Unilab, Ajax Chemicals. RPMI medium 1640 and fetal calf serum (FCS) were purchased from Invitrogen. Analytical grade (AR) chloroform ($CHCl_3$) was obtained from Merck. AR grade hexane was purchased from Univar, and AR grade methanol, ethanol, and acetone were purchased from Chem Supply. All chemicals and solvents were used as received. Milli-Q grade ($R > 18$ MΩ cm) water was used throughout.

Quantum Dot Phase Transfer. CdSe/ZnS core/shell QDs were synthesized according to previously reported methods.[37,38] QDs were transferred into aqueous media employing either (i) PSMA/EA, (ii) PSMA/M1000, (iii) PMAO/EA, or (iv) DHLA-PEG (PEG, $n = 12$), the synthesis of which is described elsewhere.[21]

PSMA/EA. QDs (50 nmol) in $CHCl_3$ were added to 5 μmol PSMA predissolved in $CHCl_3$ to give a 100-fold molar excess of PSMA. The reaction mixture (~1 mL) was tumbled at room temperature (RT) for at least 3 h. A 2 mL portion of water containing ~20 μL EA was added to the QD/PSMA $CHCl_3$ solution and tumbled for 30 min at RT, after which time the QDs had transferred into the water phase with ~100% efficiency. The sample was centrifuged at 7000 rpm for 5 min to speed up the separation of the $CHCl_3$ and water phases. The aqueous QD solution was extracted and passed through a 0.22 μm filter.

PSMA/M1000. To obtain PSMA/M1000 capped QDs, the QDs were first capped with PSMA as outlined above. M1000 dissolved in $CHCl_3$ was added to the QD/PSMA solution. Samples with molar ratios of M1000: maleic anhydride (MA) ranging from 1:5 to 5:5 were prepared assuming ~32 wt % MA. (The Sigma-Aldrich product contains 68 wt % styrene: 32 wt % MA in the polymer chain. Therefore 5 μmol (8.5 mg) PSMA contains 27 μmol (2.7 mg) MA.). As an example, for 20% of the MA groups to be ring opened with M1000 (M1000: MA, 1:5) in a 50 nmol QD/5 μmol PSMA solution, 5.5 μmol M1000 was required. The reaction mixture (~1.5 mL) was tumbled overnight at RT. A 2−3 mL portion of water was added to the QD/PSMA/M1000 $CHCl_3$ solution with ~ 20 μL EA to ring open any remaining MA groups. The solution was tumbled for 30 min at RT. $CHCl_3$ was removed by rotary evaporation to yield a turbid QD H_2O solution. 2−3 mL of fresh $CHCl_3$ was added to the QD H_2O mixture and tumbled for 3 h at RT to back-extract any hydrophobic ligands. The sample was centrifuged at 7000 rpm for 5 min in order to speed up the separation of the $CHCl_3$ and water phases. The QD H_2O solution was extracted and passed through a 0.22 μm filter.

It is noteworthy that for samples with a 1:1 or excess M1000:MA ratio, addition of EA aided the phase transfer into water. The EA acts as a base and deprotonates the PSMA carboxyl groups generated from the ring-opening of the maleic anhydride moieties and can be substituted with TMAOH or NaOH.

PMAO/EA. QDs (50 nmol) in $CHCl_3$ were added to 500 nmol PMAO predissolved in $CHCl_3$ to give a 10-fold molar excess of PMAO. The reaction mixture (~1 mL) was tumbled overnight at RT. A 2 mL portion of water containing ~20 μL EA was added to the QD/PMAO $CHCl_3$ solution and tumbled for 30 min at RT. $CHCl_3$ was removed by rotary evaporation to yield a turbid QD H_2O solution. A 2−3 mL portion of fresh $CHCl_3$ was added to the QD H_2O mixture and tumbled for 3 h at RT to back extract any hydrophobic ligands. The sample was centrifuged at 7000 rpm for 5 min in order to speed up the separation of the $CHCl_3$ and water phases. The QD H_2O solution was extracted and passed through a 0.22 μm filter.

DHLA-PEG. To obtain DHLA-PEG-capped QDs, the QDs were first transferred into water using PsAA. Approximately 7.5 nmol QDs in $CHCl_3$ were precipitated with methanol/acetone and redispersed in a 0.1 M PsAA/methanol solution where the pH had been adjusted to 8 using TMAOH. The QD/PsAA solution was heated to 60 °C overnight, precipitated with hexane/ethanol and redispersed in water. A 10000 molar excess of DHLA-PEG was added to the QD/PsAA solution and heated to 60 °C overnight.

All QD samples in aqueous media were purified or buffer exchanged into phosphate buffered saline (PBS) using an ultracentrifugal filtration device (Vivaspin, 50 kDa MWCO) with a minimum of three cycles of concentration/dilution to remove any excess ligands.

Quantum Dot Characterization. Absorption spectra were recorded on a Cary 5 UV−vis−NIR spectrophotometer. Steady-state photoluminescence spectra were recorded on a Fluorolog-3 spectrofluorimeter (Horiba Jobin Yvon) with slit widths of 1 nm and an integration time of 1 s. Concentrations were adjusted such that the QD samples had optical densities of >0.1 at the excitation wavelength. Wavelengths of 385, 400, 475, and 515 nm were used to excite quantum dot samples with first absorption maxima of 459, 509, 563, and 623 nm, respectively.

Samples were separated in a 1% agarose gel buffered with 1× tris-borate EDTA (TBE) buffer, pH 8, and run at 100 V for 45 min. A 20 μL portion of 1 μM QD samples mixed with 30% glycerol was loaded per well. Gel shift bands were visualized using a transilluminator (Syngene) with UV light excitation.

Dynamic light scattering (DLS) was employed to measure the hydrodynamic diameters of water-soluble QDs capped with different surface chemistries. QD samples (100 nM) in PBS were analyzed using a high performance particle sizer (HPPS, Malvern Instruments) operated at 25 °C. All measurements were performed in triplicate.

Cell Staining. LIM1215 human colon carcinoma cells[39] were seeded onto coverslips in six well plates and grown to confluency in RPMI 1640 media with ADDS (2 μM hydrocortisone, 10 μM thioglycerol, 100 nM insulin) supplemented with penicillin (60 μg/mL), streptomycin (100 μg/mL), and 10% FCS at 37 °C in 5% CO_2. Cells were washed with PBS (1 × 5 mL), fixed with 4% PFA for 15 min, washed again with PBS (1 × 5 mL), and blocked with 2% BSA/PBS overnight at 4 °C. Cells were washed with PBS (1 × 5 mL) and stained with 750 μL of a 1 μM QD (first absorp-

tion maxima at 582 nm) PBS solution for 30 min at RT. Cells were washed 3−5 times with PBS (5 min each). Cells were imaged using a Nikon TE2000-E inverted microscope fitted with a 60× water immersion lens (Nikon, Plan APO, NA 1.2, VC). Fluorescence images were collected using a TRITC fluorescence filter cable (Nikon, excitation 540BP25, emission 605BP55) with 2 s exposure times. Images were acquired using a Roper CoolSNAP HQ camera (Roper Scientific).

Acknowledgment. The authors thank Jenny Catimel for providing the LIM1215 human carcinoma cells. E. Lees thanks the Australian Government for support through an APA scholarship. P. Mulvaney acknowledges support through DEST ISL program grant CG 110036.

REFERENCES AND NOTES

1. Bruchez, M.; Moronne, M.; Gin, P.; Weiss, S.; Alivisatos, A. P. Semiconductor Nanocrystals as Fluorescent Biological Labels. *Science* **1998**, *281*, 2013–2016.
2. Chan, W. C. W.; Nie, S. M. Quantum Dot Bioconjugates for Ultrasensitive Nonisotopic Detection. *Science* **1998**, *281*, 2016–2018.
3. Dubertret, B.; Skourides, P.; Norris, D. J.; Noireaux, V.; Brivanlou, A. H.; Libchaber, A. *In Vivo* Imaging of Quantum Dots Encapsulated in Phospholipid Micelles. *Science* **2002**, *298*, 1759–1762.
4. Dahan, M.; Levi, S.; Luccardini, C.; Rostaing, P.; Riveau, B.; Triller, A. Diffusion Dynamics of Glycine Receptors Revealed by Single-Quantum Dot Tracking. *Science* **2003**, *302*, 442–445.
5. Wu, X. Y.; Liu, H. J.; Liu, J. Q.; Haley, K. N.; Treadway, J. A.; Larson, J. P.; Ge, N. F.; Peale, F.; Bruchez, M. P. Immunofluorescent Labeling of Cancer Marker Her2 and Other Cellular Targets with Semiconductor Quantum Dots. *Nat. Biotechnol.* **2003**, *21*, 41–46.
6. Ballou, B.; Lagerholm, B. C.; Ernst, L. A.; Bruchez, M. P.; Waggoner, A. S. Noninvasive Imaging of Quantum Dots in Mice. *Bioconjugate Chem.* **2004**, *15*, 79–86.
7. Kim, S.; Lim, Y. T.; Soltesz, E. G.; De Grand, A. M.; Lee, J.; Nakayama, A.; Parker, J. A.; Mihaljevic, T.; Laurence, R. G.; Dor, D. M.; Cohn, L. H.; Bawendi, M. G.; Frangioni, J. V. Near-Infrared Fluorescent Type II Quantum Dots for Sentinel Lymph Node Mapping. *Nat. Biotechnol.* **2004**, *22*, 93–97.
8. Clapp, A. R.; Medintz, I. L.; Mattoussi, H. Forster Resonance Energy Transfer Investigations Using Quantum-Dot Fluorophores. *ChemPhysChem* **2006**, *7*, 47–57.
9. Murray, C. B.; Norris, D. J.; Bawendi, M. G. Synthesis and Characterization of Nearly Monodisperse CdE (E = S, Se, Te) Semiconductor Nanocrystallites. *J. Am. Chem. Soc.* **1993**, *115*, 8706–8715.
10. Yu, W. W.; Peng, X. G. Formation of High-Quality CdS and other II−VI Semiconductor Nanocrystals in Noncoordinating Solvents: Tunable Reactivity of Monomers. *Angew. Chem., Int. Ed.* **2002**, *41*, 2368–2371.
11. Talapin, D. V.; Rogach, A. L.; Kornowski, A.; Haase, M.; Weller, H. Highly Luminescent Monodisperse CdSe and CdSe/ZnS Nanocrystals Synthesized in a Hexadecylamine−Trioctylphosphine Oxide−Trioctylphospine Mixture. *Nano Lett.* **2001**, *1*, 207–211.
12. van Embden, J.; Mulvaney, P. Nucleation and Growth of CdSe Nanocrystals in a Binary Ligand System. *Langmuir* **2005**, *21*, 10226–10233.
13. Jasieniak, J.; Bullen, C.; van Embden, J.; Mulvaney, P. Phosphine-free Synthesis of CdSe Nanocrystals. *J. Phys. Chem. B* **2005**, *109*, 20665–20668.
14. Willard, D. M.; Carillo, L. L.; Jaemyeong, J.; Van Orden, A. CdSe-ZnS Quantum Dots as Resonance Energy Transfer Donors in a Model Protein-Protein Binding Assay. *Nano Lett.* **2001**, *1*, 469–474.
15. Mitchell, G. P.; Mirkin, C. A.; Letsinger, R. L. Programmed Assembly of DNA Functionalized Quantum Dots. *J. Am. Chem. Soc.* **1999**, *121*, 8122–8123.
16. Hoshino, A.; Fujioka, K.; Oku, T.; Nakamura, S.; Suga, M.; Yamaguchi, Y.; Suzuki, K.; Yasuhara, M.; Yamamoto, K. Quantum Dots Targeted to the Assigned Organelle in Living Cells. *Microbiol. Immunol.* **2004**, *48*, 985–994.
17. Aldana, J.; Wang, Y. A.; Peng, X. G. Photochemical Instability of CdSe Nanocrystals Coated by Hydrophilic Thiols. *J. Am. Chem. Soc.* **2001**, *123*, 8844–8850.
18. Jiang, W.; Mardyani, S.; Fischer, H.; Chan, W. C. W. Design and Characterization of Lysine Cross-Linked Mercapto-acid Biocompatible Quantum Dots. *Chem. Mater.* **2006**, *18*, 872–878.
19. Mattoussi, H.; Mauro, J. M.; Goldman, E. R.; Anderson, G. P.; Sundar, V. C.; Mikulec, F. V.; Bawendi, M. G. Self-Assembly of CdSe−ZnS Quantum Dot Bioconjugates Using an Engineered Recombinant Protein. *J. Am. Chem. Soc.* **2000**, *122*, 12142–12150.
20. Goldman, E. R.; Balighian, E. D.; Mattoussi, H.; Kuno, M. K.; Mauro, J. M.; Tran, P. T.; Anderson, G. P. Avidin: A Natural Bridge for Quantum Dot-Antibody Conjugates. *J. Am. Chem. Soc.* **2002**, *124*, 6378–6382.
21. Uyeda, H. T.; Medintz, I. L.; Jaiswal, J. K.; Simon, S. M.; Mattoussi, H. Synthesis of Compact Multidentate Ligands to Prepare Stable Hydrophilic Quantum Dot Fluorophores. *J. Am. Chem. Soc.* **2005**, *127*, 3870–3878.
22. Susumu, K.; Uyeda, H. T.; Medintz, I. L.; Pons, T.; Delehanty, J. B.; Mattoussi, H. Enhancing the Stability and Biological Functionalities of Quantum Dots *via* Compact Multifunctional Ligands. *J. Am. Chem. Soc.* **2007**, *129*, 13987–13996.
23. Liu, W.; Howarth, M.; Greytak, A.; Zheng, Y.; Nocera, D.; Ting, A.; Bawendi, M. Compact Biocompatible Quantum Dots Functionalized for Cellular Imaging. *J. Am. Chem. Soc.* **2008**, *130*, 1274–1284.
24. Bentzen, E. L.; Tomlinson, I. D.; Mason, J.; Gresch, P.; Warnement, M. R.; Wright, D.; Sanders-Bush, E.; Blakely, R.; Rosenthal, S. J. Surface Modification to Reduce Nonspecific Binding of Quantum Dots in Live Cell Assays. *Bioconjugate Chem.* **2005**, *16*, 1488–1494.
25. Gao, X.; Chan, W. C. W.; Nie, S. Quantum-Dot Nanocrystals for Ultrasensitive Biological Labeling and Multicolor Optical Encoding. *Biomed. Opt.* **2002**, *7*, 532–537.
26. Bullen, C.; Mulvaney, P. The Effects of Chemisorption on the Luminescence of CdSe Quantum Dots. *Langmuir* **2006**, *22*, 3007–3013.
27. Gerion, D.; Pinaud, F.; Williams, S. C.; Parak, W. J.; Zanchet, D.; Weiss, S.; Alivisatos, A. P. Synthesis and Properties of Biocompatible Qater-Soluble Silica-Coated CdSe/ZnS Semiconductor Quantum Dots. *J. Phys. Chem. B* **2001**, *105*, 8861–8871.
28. Nann, T.; Mulvaney, P. Single Quantum Dots in Spherical Silica Particles. *Angew. Chem., Int. Ed.* **2004**, *43*, 5393–5396.
29. Correa-Duarte, M. A.; Giersig, M.; Liz-Marzan, L. M. Stabilization of CdS Semiconductor Nanoparticles Against Photodegradation by a Silica Coating Procedure. *Chem. Phys. Lett.* **1998**, *286*, 497–501.
30. Pellegrino, T.; Manna, L.; Kudera, S.; Liedl, T.; Koktysh, D.; Rogach, A. L.; Keller, S.; Radler, J.; Natile, G.; Parak, W. J. Hydrophobic Nanocrystals Coated with an Amphiphilic Polymer Shell: A General Route to Water Soluble Nanocrystals. *Nano Lett.* **2004**, *4*, 703–707.
31. Gao, X. H.; Cui, Y. Y.; Levenson, R. M.; Chung, L. W. K.; Nie, S. M. *In Vivo* Cancer Targeting and Imaging with Semiconductor Quantum Dots. *Nat. Biotechnol.* **2004**, *22*, 969–976.
32. Yu, W. W.; Chang, E.; Falkner, J. C.; Zhang, J. Y.; Al-Somali, A. M.; Sayes, C. M.; Johns, J.; Drezek, R.; Colvin, V. L. Forming Biocompatible and Nonaggregated Nanocrystals in Water Using Amphiphilic Polymers. *J. Am. Chem. Soc.* **2007**, *129*, 2871–2879.
33. Lin, C. J.; Sperling, R. A.; Li, J. K.; Yang, T.; Li, P.; Zanella, M.; Chang, W. H.; Parak, W. J. Design of an Amphiphilic Polymer for Nanoparticle Coating and Functionalization. *Small* **2008**, *4*, 334–341.
34. Anderson, R. E.; Chan, W. C. W. Systematic Investigation of Preparing Biocompatible, Single, and Small ZnS-Capped

CdSe Quantum Dots with Amphiphilic Polymers. *ACS Nano* **2008**, *2*, 1341–1352.
35. Choi, H. S.; Liu, W.; Misra, P.; Tanaka, E.; Zimmer, J. P.; Ipe, B. I.; Bawendi, M. G.; Frangioni, J. V. Renal Clearance of Quantum Dots. *Nat. Biotechnol.* **2007**, *25*, 1165–1170.
36. Smith, A. M.; Nie, S. Nanocrystal Synthesis in an Amphibious Bath: Spontaneous Generation of Hydrophilic and Hydrophobic Surface Coatings. *Angew. Chem., Int. Ed.* **2008**, *47*, 9916–9921.
37. Li, J. J.; Wang, Y. A.; Guo, W. Z.; Keay, J. C.; Mishima, T. D.; Johnson, M. B.; Peng, X. G. Large-Scale Synthesis of Nearly Monodisperse CdSe/CdS Core/Shell Nanocrystals using Air-Stable Reagents *via* Successive Ion Layer Adsorption and Reaction. *J. Am. Chem. Soc.* **2003**, *125*, 12567–12575.
38. van Embden, J.; Jasieniak, J.; Gomez, D. E.; Mulvaney, P.; Giersig, M. Review of the Synthetic Chemistry Involved in the Production of Core/Shell Semiconductor Nanocrystals. *Aust. J. Chem.* **2007**, *60*, 457–471.
39. Whitehead, R. H.; Macrae, F. A.; St. John, D. J.; Ma, J. A. Colon Cancer Cell-Line (LIM1215) Derived From a Patient with Inherited Nonpolyposis Colorectal-Cancer. *J. Natl. Cancer Inst.* **1985**, *74*, 759–765.